EVALUATION OF THE HEAVY METALS MERCURY, LEAD AND ARSENIC IN ATMOSPHERIC PARTICULATES OF TABBIN RESIDENTIAL AREA, CAIRO, EGYPT

Marwa O. Kosbar[(1)]; Nabil A. Saleh[(2)]; Mahmoud A. Hewehy[(1)]; Naga A. Abou Alnel[(3)]; Waleed A. Abbas[(3)]

1) Department of Basic Environmental Sciences, Faculty of Environmental Studies and Research, Ain Shams University, Cairo, Egypt, Marwa.Kosbar@iesr.asu.edu.eg
2) Department of Biochemistry, Faculty of Science, Ain Shams University, Cairo, Egypt
3) Department of Geography and GIS, Faculty of Arts, Ain Shams University, Cairo, Egypt, waleed.abbas@art.asu.edu.eg

ABSTRACT

At three selected residential locations in Tabbin area, seasonal samples of airborne heavy metal concentrations were analyzed, and results interpreted. Heavy metals of mercury (Hg), lead (Pb), and arsenic (As) in particulate matter with an aerodynamic diameter of ten micrometer or less (PM10) were assessed. The work depended entirely on collecting in-situ 36 air samples, 12 per location during 2022–2023. The analysis of particulate matter and its heavy metal concentrations across separate locations revealed a complex environmental landscape. PM10 levels fluctuated significantly at Location 01, while Location 03 experienced sporadic spikes, indicating episodic pollution events. Arsenic was high at Location 01, contrasting with the low levels found at Location 02. Mercury's noticeable rise at location 03 indicated that emissions from the cement industry nearby were caused by burning coal. Meanwhile, elevated Pb levels at Location 02 indicated such activities and production emissions of specific local sources, including traffic congestion, smelters, and foundries. PM10 variations did not show any significant mean difference across locations, but the disparities in heavy metal concentrations were pronounced. This conclusion underscores the need for adopting extensive source apportionment, environmental assessments and confrontation plans by the local governments and research institutions.

Keywords: Particulate matter (PM10), Mercury, Lead, Arsenic, Tabbin, residential locations.

INTRODUCTION

Air pollution, particularly including particulate matter (PM), is a crucial environmental and human health issue, especially in densely populated urban areas (Manisalidis *et al.*, 2020). Among various air pollutants, particulate matter with an aerodynamic diameter of 10 micrometers or less (PM10) has environmental and health concern due to their small size,

Vol. (54); No. (2); Feb. 2025
Print ISSN 1110-0826
Online ISSN 2636 - 3178

ability to penetrate the respiratory system, and their association with severe health outcomes, including respiratory and cardiovascular diseases, as well as carcinogenic effect (Alemayehu *et al.,* 2020; Kyung and Jeong, 2020; Basith *et al.*, 2022).

In the Middle East and North Africa (MENA) region, air pollution levels are rising due to arid climate and unplanned urbanization including industrialization, congested vehicular traffic (Imane *et al.,* 2022; Fadel *et al.,* 2023; Isaifan and Al-Thani, 2024). The World Health Organization (WHO) uses the annual average of PM to evaluate ambient air quality. From 2011 to 2015, Cairo, the capital of Egypt, was one of the highly polluted cities in the MENA area, with PM10 levels above 150 μg/m^3 (WHO, 2016).

Previous studies indicated alarming levels of PM over various sites in Cairo, especially in mixed residential—industrial areas due to a combination of local industrial activities, vehicles emissions, open burning, and geological material and natural sources (Abu-allaban *et al.,* 2007; Abbas *et al.,* 2020; Hwehy *et al.,* 2024). In accordance with funding from Denmark and the United States, the Egyptian Environmental Affairs Agency (EEAA) launched a monitoring program to identify temporal and regional changes in pollutant concentrations since 1998 and numerous observation points were established (Safar and Labib, 2010). Pb and ambient PM (PM10 and PM2.5) were monitored via the USAID-funded Cairo Air Improvement Project (CAIP). In addition, the levels of toxic gases (SO_2, NO_2, CO, and O_3) were recorded via the DANIDA-funded Egyptian Information and Monitoring Program (EIMP) (Sivertsen, 2004). Furthermore, several studies (Elmotily *et al.,* 2021; Elawa and Farahat, 2022) that were conducted to examine the air quality over Cairo assessed the ambient air quality levels at various locations in Cairo. The airborne heavy metals in urban environments are concerned because of their toxic properties and persistence in the environment (Borai and Soliman, 2001). Shetaya *et al.* (2024) investigated the PM2.5 air concentrations and associated heavy metals, including Pb, at two sites (Tabbin and Dokki). They found that Pb posed the greatest health threat in (Greater Cairo). While inhalation was a significant exposure route for non-carcinogenic risks for all elements combined and some individual elements. Monged *et al.* (2022) evaluated the presence of heavy metals in airborne PM10 at two residential sites in Giza and Helwan (Greater Cairo).

They concluded that the carcinogenic and non-carcinogenic risks from inhaling these heavy metals for both children and adults were below the safe limits at both sites.

Some studies evaluated the heavy metals in the road dust (Abdel-Latif and Saleh, 2012; Hegazy *et al.*, 2024) and found significant contamination with heavy metals. Their findings indicate that road dust is heavily contaminated with Pb. The heavy metal content and spatial distribution of road dust in Cairo reported an average Pb concentration of 1798 ppm. These results were particularly evident in heavy traffic and industrial areas, showing a remarkably high degree of contamination and unfavorable health drawbacks.

The current paper aims to provide a comprehensive assessment of airborne heavy metals in PM10 in high densely populated areas close to Tabbin industrial complex in Cairo, Egypt. The outcoming findings will help a deeper understanding of current levels of heavy metals pollution, which provides critical data for policymakers and stakeholders aiming to mitigate public health risks.

MATERIALS AND METHODS

This section shows the selected study area, location of sampling, sampling methodology, sampling schedule, equipment, chemical analysis method, and statistical analysis used.

Area of study:

Tabbin is a heavily populated industrial-residential district located south of Cairo, Egypt. Steel, cement, fertilizer, mining, and coke production heavy industries surround the residential district. In the residential area of Tabbin, three sampling sites were chosen. These were residential buildings in the area, major roads are close by at site 2, and an open area is close by at location 3. To collect the PM10 sample monthly to be analyzed for the selected heavy-metal content. Figure 1 shows the locations map and indicates the surrounding main industries and boundaries of residential areas. The three locations are located downwind of the metal, cement, and steel production facilities. Location 01 is in the highly populated area inside Tabbin. Location 02 is highly crowded and contains main roads conjugated between different areas. Location 03 is a less populated area with less traffic and crowded.

Vol. (54); No. (2); Feb. 2025
Print ISSN 1110-0826
Online ISSN 2636 - 3178

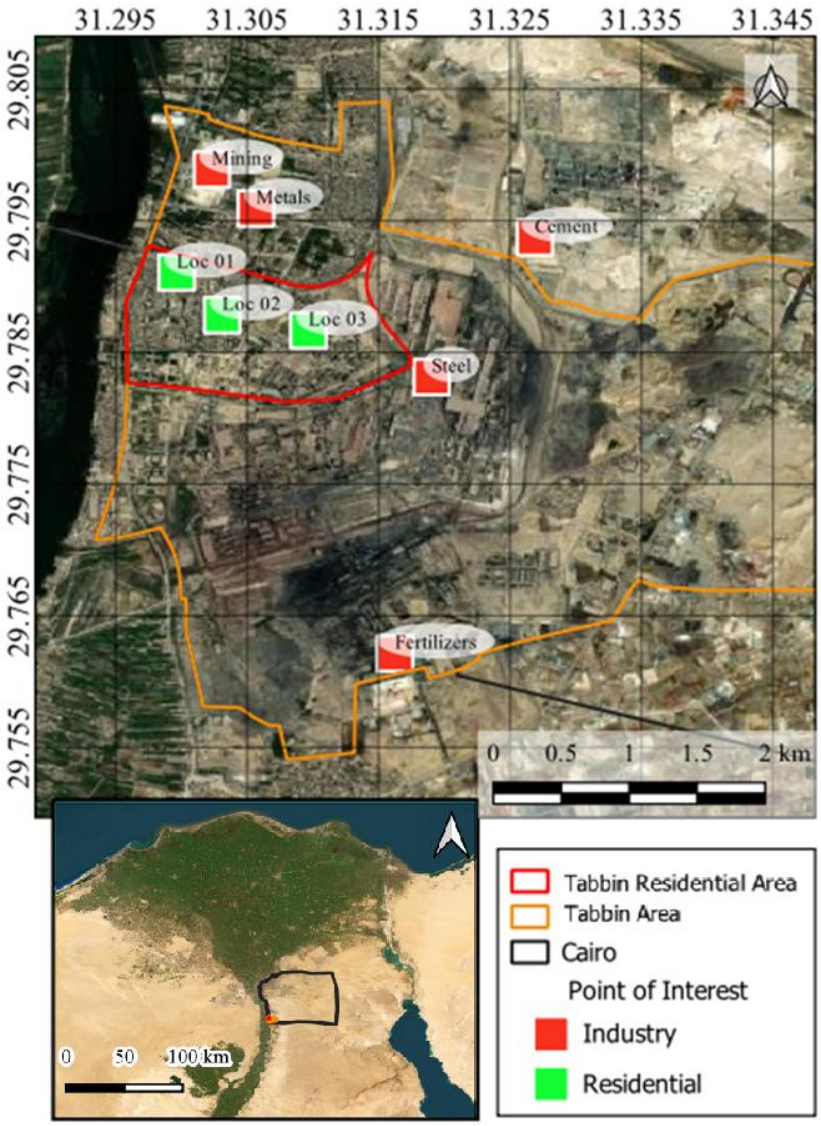

Figure 1. Satellite image of study area

- Green squares represent the sampling locations in the residential area of Tabbin, while red squares represent common industrial effective sources.
- (Amended after ESRI IMAGERY)

Vol. (54); No. (2); Feb. 2025
Print ISSN 1110-0826
Online ISSN 2636 - 3178

1.1. Sampling

Twelve samples for each location were collected during the schedule shown in Table 1. Three air samplers were used at the same time to collect a 24-hour sample of PM10 for each location. All samples were located approximately 10 meters above ground level on the building roofs. The sampling methodology follows U.S. Environmental Protection Agency (USEPA) compendium method IO-2.3 for sampling of ambient air PM10 using low volume sampler. USEPA's compendium method IO-3.4 was used to determine the metals in ambient PM10 using Inductive Coupled Plasma (ICP) spectroscopy (USEPA, 1999a; USEPA, 1999b).

Table 1. Sampling* Schedule all over the period of study (4 seasons).

YEAR	SEASON	MONTH	START	END
2022	Summer	July	Friday, 1st	Saturday, 2nd
		August	Friday, 5th	Saturday, 6th
		September	Friday, 2nd	Saturday, 3rd
	Autumn	October	Friday, 7th	Saturday, 8th
		November	Friday, 4th	Saturday, 5th
		December	Friday, 2nd	Saturday, 3rd
2023	Winter	January	Friday, 6th	Saturday, 7th
		February	Friday, 3rd	Saturday, 4th
		March	Friday, 3rd	Saturday, 4th
	Spring	April	Friday, 7th	Saturday, 8th
		May	Friday, 5th	Saturday, 6th
		June	Friday, 9th	Saturday, 10th
The sampling program started from Friday 1st of July 2022 till Saturday,10th of June 2023. *The sampling time is 24 hours for each location. Each location has different start and end hours during start and end days of sampling.				

1.1.1. Equipment

Mini-volume air samplers, AIRMETRICS, USA, were used to collect a 24-hour PM10 sample at each location. Watman glass microfiber 47 mm filters suitable for PM10 sampling and heavy metals analysis were used. Filters were held on stainless steel support screens in 47 mm filter cassette. Then filter cassette with glass filter installed in filter holder which

Vol. (54); No. (2); Feb. 2025
Print ISSN 1110-0826
Online ISSN 2636 - 3178

includes a PM10 impactor designed to separate PM10 at a flow rate of 5L/minute. Each filter was weighed using a four-digit balance. Heavy metals are determined using ICP-optical emission spectroscopy (ICP-OES), manufactured by Perkin Elmer, USA, and owned by Holding Company for water and wastewater, Reference laboratory for drinking water.

1.1.2. Chemicals

The filter was digested using 100 ml of 2% nitric acid (HNO3) ultra grade to extract heavy metals (USEPA, 1999a).

1.1.3. Calculations

PM10 sample concentration was calculated using equation 1 (USEPA, 1999a):

$PM10 = (W_f - W_i) / V_{sd}$ (*eq. 1)*

Where: PM is average mass concentration ($\mu g/m^3$), W_i is average final weight of exposed filter (µg), W_f is average initial weight of clean filter (µg), and V_{sd} is the sampled volume drawn through the filter, corrected to standard temperature.

Airborne heavy metal concentration in the air sample was calculated using equation 2 (USEPA, 1999b):

Metal ($\mu g/m^3$) = (µg metal /L) × (final extraction volume L)/ V_{sd} (*eq. 2)*

1.2. Heavy metal

The serious health effects of mercury (Hg), lead (Pb), and arsenic (As) make them top priorities in environmental studies. Arsenic's carcinogenic dangers and mercury's neurotoxicity and biomagnification highlight their significance. Mercury causes cardiovascular and neurodevelopmental issues. Important public health issues were addressed by monitoring these metals, especially in areas where humans have an impact and in polluted ecosystems. Additionally, these heavy metals are linked to nearby industrial operations and vehicle emissions (Rahman and Singh, 2019).

1.3. Weather data

The weather has a considerable influence on the dispersion of pollutants (Mohamed et al., 2023). Weather observations data were obtained for a similar duration from the Iowa State University - Iowa Environmental Mesonota database of archives of automated airport weather observations Automated Surface Observing System (Herzmann and Wolt, 2020).

Vol. (54); No. (2); Feb. 2025
Print ISSN 1110-0826
Online ISSN 2636 - 3178

Figures 2–5 show the wind rose plots of the wind speed and wind direction for the sampling duration. The direction of the wind is represented by the angle and the length of the cone represent the frequency (%), while the colored code represents the speed categories.

The prevalent direction is the northern wind during summer and autumn months. The high variation of wind direction during winter and spring months indicates a meso-seasonal wind and depression. High wind speeds in April and May could cause the natural road dust to be ploughed. Otherwise, the slow wind in January and March refers to a stable atmospheric condition that results in high concentrations and pollutant deposition.

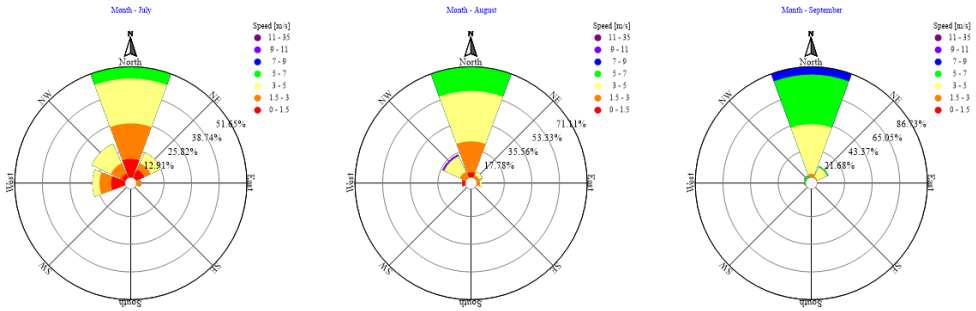

Figure 2. Monthly wind rose plots during sampling days of period from July to September 2022.

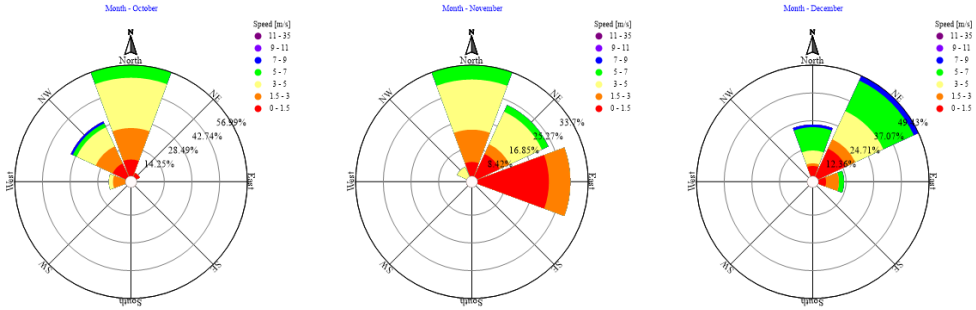

Figure 3. Monthly wind rose plots during sampling days of period from October to December 2022.

Vol. (54); No. (2); Feb. 2025
Print ISSN 1110-0826
Online ISSN 2636 - 3178

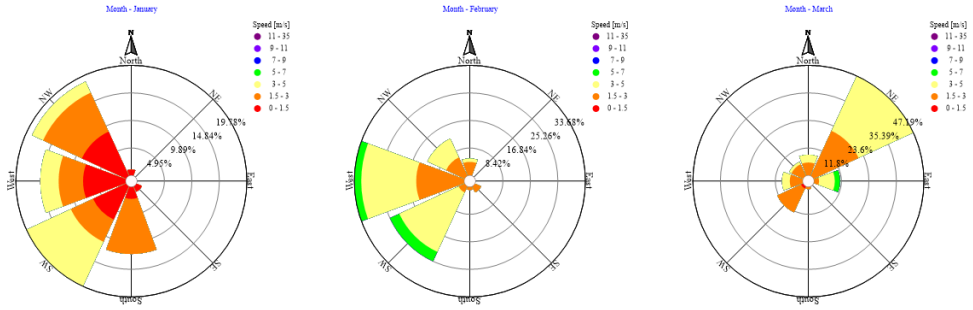

Figure 4. Monthly wind rose plots during sampling days of period from January to March 2023.

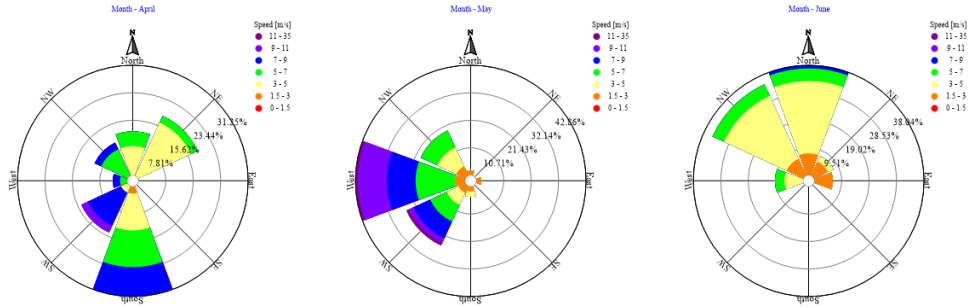

Figure 5. Monthly wind rose plots during sampling days of period from April to June 2023.

1.4. Statistical analysis

In the assessment of PM10 and heavy metal concentration levels, statistical analysis plays a crucial role in interpreting and understanding the data collected from the three sampling locations. Descriptive statistics, including measures of central tendency (mean) and dispersion (variation, standard deviation, and standard error), provide insights into the concentration levels and variability of PM10 and heavy metals. The standard deviation is crucial in identifying the spread of the data around the mean, allowing for an understanding of how consistent or fluctuating the pollutant concentrations are across the dataset. Furthermore, hypothesis testing using the independent sample t-test can be employed to determine whether there is a statistically significant difference in mean concentrations between different sampling sites. This helps to understand spatial variability and identify locations with potentially higher pollution levels. In addition, wind rose plots are

Vol. (54); No. (2); Feb. 2025
Print ISSN 1110-0826
Online ISSN 2636 - 3178

instrumental in analyzing the influence of wind during the sampling period. By illustrating the frequency and direction of wind, these diagrams help correlate wind patterns with pollutant dispersion, offering critical insights into the transport of PM10 and heavy metals from potential emission sources. Together, these statistical tools and visual aids provide a robust framework for understanding the spatial and temporal variability of air pollution levels in each location.

RESULTS

The findings of samples are statistically described in Table 2. Figures 6–9 represent the seasonal variation. PM10 concentrations data for the three investigated locations provide a range from 74 µg/m³ (minimum) to 275 µg/m³ (maximum), from 53 µg/m³ to 255 µg/m³, and 108 µg/m³ to 274 µg/m³ for locations 1, 2, and 3, respectively. The median exceeded the Egyptian regulation limits, 150 µg/m³ for 24-hour limits.

The mean concentration is 171 µg/m³, closely aligned with the median value of 172 µg/m³, suggesting a symmetric distribution of PM10 values in location 01. The slight skewness at Location 03, indicated by the difference between the mean and median, suggests potential higher concentration events that may have influenced the overall mean such as high wind speed and dust events during spring.

Data from the three locations present a detailed analysis of arsenic concentrations in the air. At Location 01, arsenic levels ranged from 0.042 to 0.081 µg/m³, with a mean of 0.059 µg/m³ and a median of 0.056 µg/m³, indicating a symmetrical distribution with moderate variability. Location 02 displayed lower arsenic concentrations, with values spanning from 0.024 to 0.048 µg/m³ and an average of 0.033 µg/m³ closely aligned with the median of 0.031 µg/m³, suggesting a similar distribution pattern to Location 01 but at reduced levels. In contrast, Location 03 had a wider range of arsenic concentrations, from 0.020 to 0.082 µg/m³, with a mean of 0.043 µg/m³ and a median value of 0.042 µg/m³, reflecting a symmetrical distribution but with notable variability. These findings are crucial for understanding the environmental arsenic exposure and assessing potential health risks associated with air quality in these areas.

Vol. (54); No. (2); Feb. 2025
Print ISSN 1110-0826
Online ISSN 2636 - 3178

Arsenic concentrations are higher on average at Location 01, while Location 02, which was located in a congested building area, has the lowest average and range of its concentrations. Location 03 falls in between the two locations in terms of average concentrations but shows a broader range, with a higher maximum value compared to Location 02.

In a comparative analysis of mercury concentrations across three distinct locations, we observe a range of distribution patterns and levels. Location 01 exhibits a moderate spread in mercury levels, with concentrations ranging from 0.015 to 0.035 µg/m³ and an average close to the median, indicating a symmetrical distribution. Location 02 presents a narrower range of mercury values, from 0.016 to 0.028 µg/m³, with its mean and median identical, suggesting a highly consistent and symmetrical distribution pattern. In stark contrast, Location 03 shows significantly elevated mercury concentrations, with a minimum of 0.086 µg/m³ and a maximum of 0.137 µg/m³, far surpassing the levels found in the other locations. The proximity of the average to the median in Location 03 also denotes a symmetrical distribution, albeit at a much higher concentration range, highlighting a notable increase in mercury levels in the air at this site.

Location 03 exhibits significantly higher mercury concentrations both in terms of the range and the mean compared to Locations 01 and 02. This suggests that Location 03 may have various sources or environmental conditions contributing to these elevated mercury levels, possibly referring to the use of coal as a fossil fuel in the cement industry.

In a comparative analysis of lead concentrations across three distinct locations, the results show varying degrees of variability and distribution symmetry. Location 01 exhibits the most stable environment with lead levels ranging narrowly from 0.149 to 0.197 µg/m³, and an average almost identical to the median, suggesting a symmetric distribution. In contrast, Location 02 presents a more dynamic scenario with lead concentrations stretching from 0.416 to 0.724 µg/m³, indicating a broader variability despite a symmetric distribution pattern. Location 03 mirrors the stability of Location 01 with its lead levels spanning a modest range from 0.099 to 0.161 µg/m³; however, a slight positive skew is noted as the mean exceeds the median, hinting at occasional higher values. These observations are

Vol. (54); No. (2); Feb. 2025
Print ISSN 1110-0826
Online ISSN 2636 - 3178

crucial for understanding the environmental lead exposure and potential health implications in these areas.

Spatial assessment

Figures 6–9 show the pollutant concentration mean for each location; the findings point that Location 01 (Loc 01) recorded moderate concentrations of all heavy metals (Hg, Pb, As) across all seasons. PM10 levels fluctuated, with the highest concentrations observed in the spring (247 ± 38 µg/m³) and the lowest in summer (108 ± 39 µg/m³). Location 02 (Loc 02) demonstrated the highest levels of lead (Pb) throughout all seasons, with particularly elevated values in spring (0.668 ± 0.055 µg/m³) and autumn (0.525 ± 0.06 µg/m³). The PM10 levels at this location were lower in autumn (120 ± 62 µg/m³) but increased during winter (203 ± 39 µg/m³).

Location 03 (Loc 03) exhibited the highest concentrations of mercury (Hg) across all seasons, with spring showing the highest level (0.135 ± 0.002 µg/m³) and autumn displaying a similarly elevated concentration (0.126 ± 0.011 µg/m³). Arsenic (As) concentrations were also relatively high at this location in spring (0.068 ± 0.013 µg/m³). PM10 levels were highest in autumn (248 ± 26 µg/m³) and winter (254 ± 8 µg/m³), suggesting that this area might have significant industrial or vehicular emissions contributing to particulate matter pollution.

1.5. Temporal assessment

Table 3 shows the seasonally mean average of PM10 and heavy metal concentrations; the findings point out that in Summer, Location 03 recorded significantly higher mercury levels compared to Location 01 and Location 02 ($t = 0.001$ and 0.002, respectively, $df = 4$). Similarly, Location 02 had significantly elevated levels of lead compared to the other two locations ($t = 0.008$ and 0.002 for loc 01, and loc 03, respectively, $df = 4$), where Location 01 and Location 03 showed lower concentrations. The levels of Arsenic at all three locations varied significantly, with Location 01 being the highest, followed by Location 03, and Location 02 having the lowest ($t = 0.0001$ for each). No significant difference in PM10 was observed among the three locations ($t > 0.025$ for each).

Vol. (54); No. (2); Feb. 2025
Print ISSN 1110-0826
Online ISSN 2636 - 3178

In Autumn, Location 03 recorded significantly higher levels of Mercury (Hg) (0.126 ± 0.011 µg/m³) compared to Location 01 and Location 02, indicating greater mercury contamination in this area (t = 0.001, 0.002). There was a clear spatial variation with Location 02 showing significantly higher Lead (Pb) concentrations compared to Location 01 and Location 03 (t = 0.002, 0.003). No significant difference in Arsenic (As) among the three locations across Location 01, Location 02, and Location 03 was recorded. There was no significant difference in PM10 levels among the three locations, suggesting similar PM distribution across autumn.

Winter:

Mercury (Hg): Location 03 consistently had the highest levels, suggesting a persistent source of mercury in this location across seasons.

Lead (Pb): Location 02 had significantly higher levels, with Location 01 and Location 03 showing significantly lower concentrations.

Arsenic (As): Location 01 and Location 02 showed similar levels, while Location 03 had significantly lower concentrations.

PM10: Although PM10 levels were highest at Location 03 (254 ± 8 µg/m³), all locations showed no significant difference, indicating that PM10 variations may not be as spatially distinct.

Spring:

Mercury (Hg): Location 03 had significantly higher Hg levels (0.135 ± 0.002 µg/m³) compared to the other two locations, confirming Location 03 as a hotspot for mercury pollution.

Lead (Pb): Like autumn, Location 02 exhibited significantly elevated Pb levels, whereas Location 01 and Location 03 had significantly lower concentrations.

Arsenic (As): Location 02 had significantly lower arsenic levels compared to Location 01 and Location 03, indicating less As contamination at Location 02 during this period.

PM10: No significant differences were observed among the locations.

Vol. (54); No. (2); Feb. 2025
Print ISSN 1110-0826
Online ISSN 2636 - 3178

Table 2. Statistic description of samples results

SITE / POLLUTANT	STATISTICAL PARAMETER	LOC 01	LOC 02	LOC 03
PM10	Range	74 - 275	53 - 255	108 - 274
	Mean	171	166	196
	median	172	173	212
	±SD	67	60	64
Mercury (Hg)	Range	0.015 - 0.035	0.016 - 0.028	0.086 - 0.137
	Mean	0.024	0.022	0.119
	median	0.022	0.022	0.121
	±SD	0.007	0.004	0.016
Lead (Pb)	Range	0.150 - 0.197	0.416 - 0.724	0.099 - 0.161
	Mean	0.167	0.535	0.123
	median	0.168	0.519	0.116
	±SD	0.016	0.095	0.021
Arsenic (As)	Range	0.042 - 0.081	0.024 - 0.048	0.020 - 0.082
	Mean	0.059	0.033	0.043
	median	0.056	0.031	0.042
	±SD	0.012	0.008	0.019

- Unit of values is µg/m$^{3.}$
- (Mean=($\sum_{i=1}^{n} x_i$) / n); where "x" is the pollutant concentration, and "n" is the number of observations.

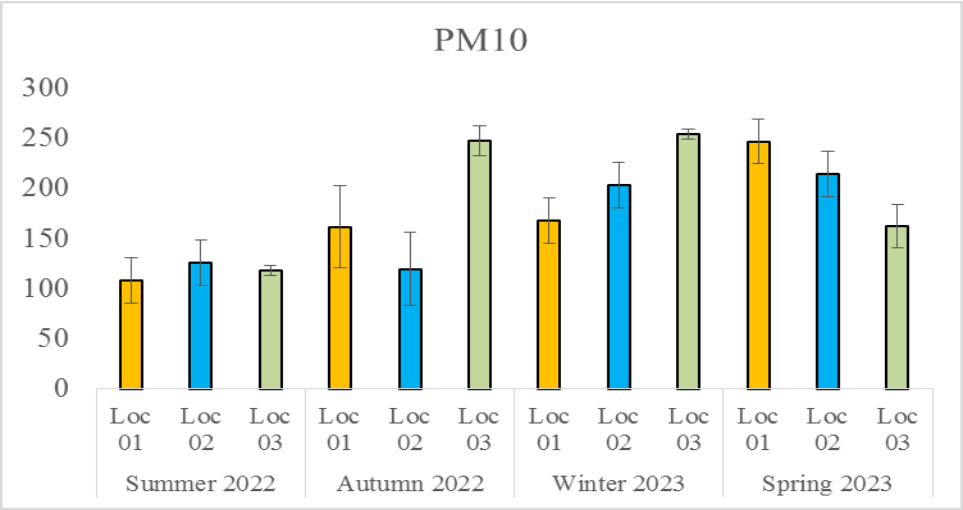

Figure 6. PM10 concentration (µg/m^3) at the study locations (Error bar represents the SE)

Vol. (54); No. (2); Feb. 2025
Print ISSN 1110-0826
Online ISSN 2636 - 3178

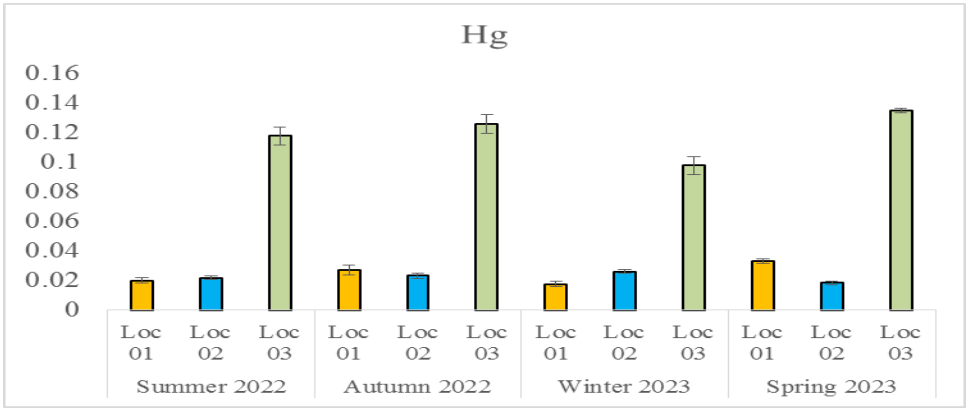

Figure 7. Mercury concentration (µg/m^3) at the study locations (Error bar represents the SE)

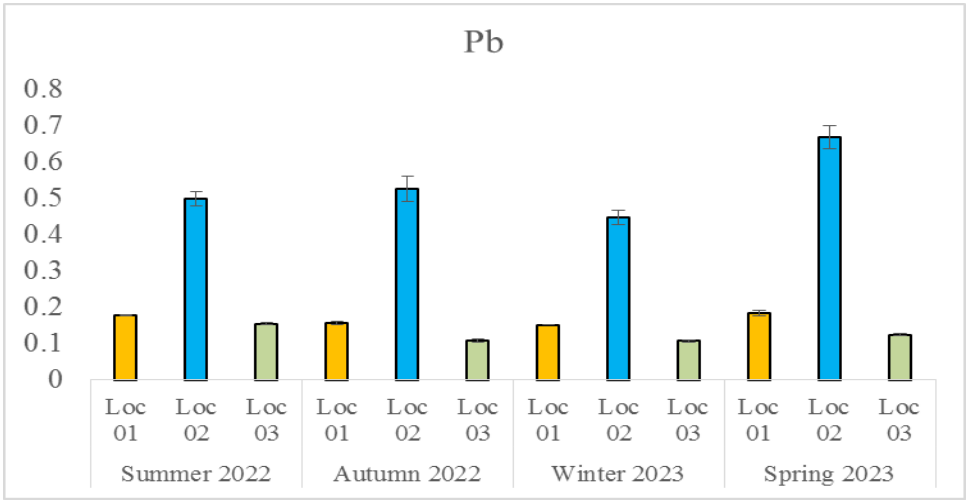

Figure 8. Lead concentration (µg/m^3) at the study locations (Error bar represents the SE)

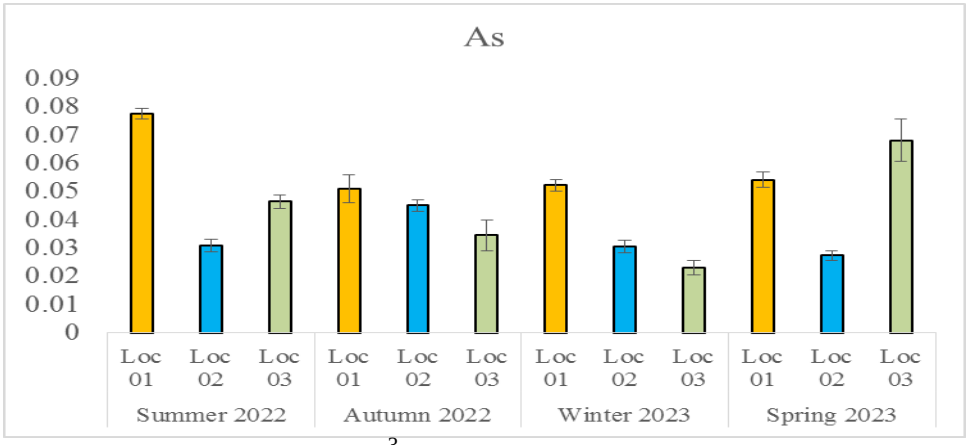

Figure 9. Arsenic concentration (µg/m^3) at the study locations (Error bar represents the SE)

Vol. (54); No. (2); Feb. 2025
Print ISSN 1110-0826
Online ISSN 2636 - 3178

Table 3. Seasonal variation in the concentration of the PM10, Hg, Pb, and as at the three studied locations (Tabbin area).

SEASON	SITE	PM10	HG	PB	AS
SUMMER 2022	Loc 01	108 ± 39 [a]	0.020 ± 0.003 [a]	0.177 ± 0.002 [a]	0.078 ± 0.003 [a]
	Loc 02	126 ± 39 [a]	0.022 ± 0.002 [a]	0.499 ± 0.036 [b]	0.031 ± 0.004 [b]
	Loc 03	118 ± 8 [a]	0.118 ± 0.010 [b]	0.154 ± 0.006 [c]	0.046 ± 0.004 [c]
AUTUMN 2022	Loc 01	162 ± 71 [a]	0.027 ± 0.006 [a]	0.155 ± 0.008 [a]	0.051 ± 0.009 [a]
	Loc 02	120 ± 62 [a]	0.023 ± 0.003 [a]	0.525 ± 0.060 [b]	0.045 ± 0.004 [a]
	Loc 03	248 ± 26 [a]	0.126 ± 0.011 [b]	0.107 ± 0.008 [c]	0.035 ± 0.009 [a]
WINTER 2023	Loc 01	168 ± 39 [a]	0.017 ± 0.003 [a]	0.152 ± 0.002 [a]	0.052 ± 0.003 [a]
	Loc 02	203 ± 39 [a]	0.026 ± 0.002 [b]	0.447 ± 0.036 [b]	0.031 ± 0.004 [a]
	Loc 03	254 ± 8 [a]	0.098 ± 0.010 [c]	0.107 ± 0.006 [c]	0.023 ± 0.004 [b]
SPRING 2023	Loc 01	247 ± 38 [a]	0.033 ± 0.003 [a]	0.184 ± 0.013 [a]	0.054 ± 0.005 [a]
	Loc 02	215 ± 40 [a]	0.018 ± 0.002 [b]	0.668 ± 0.055 [b]	0.027 ± 0.003 [b]
	Loc 03	162 ± 38 [a]	0.135 ± 0.002 [c]	0.124 ± 0.007 [c]	0.068 ± 0.013 [a]

- The values represent the mean and standard deviation.
- Distinct letters (a, b, and c) indicate a statistically significant difference in mean pollutant levels across locations for each season, whereas identical letters denote no significant difference.

DISCUSSION

Airborne heavy metals pose significant risks to both environmental and human health. Once released into the atmosphere through industrial activities, vehicular emissions, and mining operations, these metals can settle on soil and water bodies. Exposure to airborne heavy metals primarily occurs through inhalation or ingestion of contaminated food and water. Long-term exposure is associated with serious health problems, including respiratory issues, neurological disorders, cardiovascular diseases, and an increased risk of cancers Lamas *et al.* (2023).

The study's findings show that there is a considerable amount of temporal and regional fluctuation in the concentrations of PM10 and heavy metals (Hg, Pb, and As). The three locations investigated with the highest concentrations of airborne particulates with heavy metals were indicative of the causes and influencing factors of industrial pollution, this is compatible with Elawa and Farahat (2022) findings.

The wind during sampling indicates that the prevalent northern winds during summer and autumn facilitated the dispersion of pollutants, potentially reducing localized concentrations. However, the variable wind directions observed in winter and spring,

Vol. (54); No. (2); Feb. 2025
Print ISSN 1110-0826
Online ISSN 2636 - 3178

coupled with lower wind speeds, contributed to higher pollutant deposition and physical accumulation, particularly for PM10, this agrees with Hwehy *et al.* (2024). This observation aligns with the elevated PM10 concentrations recorded at Location 03 during these seasons.

The influence of wind patterns is crucial in understanding the spatial distribution of heavy metals. For instance, the elevated Pb levels at Location 02 due to high traffic impacts Abbas *et al.* (2020). The highest values during autumn and winter may be attributed to the stagnation of air masses, leading to greater pollutant accumulation from nearby sources. Similarly, high mercury levels at Location 03 suggest a possible source of cement emissions located upwind of this site, especially when wind speeds are low.

The spatial assessment indicates that each location experiences distinct levels of heavy metal pollution, likely due to the influence of local activities, wind patterns, and topographical features as found by Elmotily *et al.* (2022). The highest concentrations of Pb and Hg were consistently found at Location 02 and Location 03, respectively, highlighting the need for targeted pollution control measures in these areas to minimize these events down.

The temporal assessment revealed seasonal variations in pollutant concentrations, suggesting that meteorological factors and human activities play a critical role in shaping air quality as the finding of Mohamed *et al. (*2023). The high concentrations of heavy metals in spring and autumn can be attributed to increased human activities such as traffic, industrial emissions, and agricultural practices, combined with changes in wind patterns and speeds that affect pollutant dispersion.

This study has highlighted the intricate spatial and temporal patterns of heavy metal pollution in the urbanized Tabbin area, Cairo, emphasizing the impact of wind patterns, human activities, and seasonal variations in air quality. This reflects the risk of such communities being exposed to inhaled heavy metals and hazardous health consequences. Implementing appropriate mitigation measures is crucial for safeguarding public health and reducing environmental risks in this region.

Vol. (54); No. (2); Feb. 2025
Print ISSN 1110-0826
Online ISSN 2636 - 3178

CONCLUSION AND RECOMMENDATIONS

Conclusion

This study revealed significant spatial and temporal variations in heavy metal (Hg, Pb, and As) and PM10 concentrations across three residential locations in Tabbin, Cairo, Egypt. Elevated concentrations were observed at specific locations, influenced by wind patterns, human activities, and seasonal changes. The consistently elevated levels of lead at Location 02 and mercury at Location 03 highlight potential pollution hotspots that require immediate attention.

Recommendations

Enhanced Monitoring: Regular air quality monitoring, especially at Locations 02 and 03, to detect pollution trends and guide control measures.

Pollution Control: Stricter regulations on industrial emissions and vehicular exhaust, and traffic heaviness focusing on areas with high pollutant levels.

Public Awareness: Educate the community on pollution sources and promote practices that reduce emissions, such as using cleaner fuels and minimizing vehicle idling.

These steps will help manage heavy metal pollution, protect public health, and improve environmental quality in Tabbin area.

REFERENCES

Abbass, R., Kumar, P., and El-Gendy, A. (2020). Car users' exposure to particulate matter and gaseous air pollutants in megacity Cairo. *Sustainable Cities and Society*, 56, 102090.

Abdel-Latif, N., and Saleh, I. (2012). Heavy metals contamination in roadside dust along major roads and correlation with urbanization activities in Cairo, Egypt. *Journal of American Science*, 8(6), 379-389.

Abu-Allaban, M., Lowenthal, D., Gertler, A., and Labib, M. (2007). Sources of PM10 and PM 2.5 in Cairo's ambient air. *Environmental Monitoring and Assessment*, 133, 417-425.

Alemayehu, Y., Asfaw, S., and Terfie, T. (2020). Exposure to urban particulate matter and its association with human health risks. *Environmental Science and Pollution Research*, 27(22), 27491-27506.

Basith, S., Manavalan, B., Shin, T., Park, C., Lee, W., Kim, J., and Lee, G. (2022). The impact of fine particulate matter 2.5 on the cardiovascular system: a review of the invisible killer. *Nanomaterials*, 12(15), 2656.

Vol. (54); No. (2); Feb. 2025
Print ISSN 1110-0826
Online ISSN 2636 - 3178

Borai, E. and Soliman, A. (2001). Monitoring and statistical evaluation of heavy metals in airborne particulates in Cairo, Egypt. *Journal of Chromatography A*, 920(1-2), 261-269.

Elawa, O., and Farahat, E. (2022). Assessment of ambient air quality level at 21 sites in cement sector, Egypt. *Egyptian Journal of Chemistry*, 65(9), 47-57.

ElMotily, H., Hewehy, M., and Yousry, B. (2021). Comparison of inorganic chemical compositions of total suspended and respirable particulates in different regions of Cairo. *Journal of Environmental Science*, 50(3), 1-38.

Fadel, M., Courcot, D., Seigneur, M., Kfoury, A., Oikonomou, K., Sciare, J., and Afif, C. (2023). Identification and apportionment of local and long-range sources of PM2.5 in two East-Mediterranean sites. *Atmospheric Pollution Research*, 14(1), 101622.

Hegazy, H., Hashem, F., Maree, R., and Hewehy, M. (2024). Geochemical characterization of heavy metals and environmental risk assessment of road dust in Cairo, Egypt. *Journal of Environmental Science*, 53(4), 1082-1110.

Herzmann, D., & Wolt, J. (2020). Iowa state university Iowa Environmental Mesonet. Accessed on November 30, 2024 at *http://mesonet.agron.iastate.edu/info/nni.phtml*

Hwehy, M., Moursy, F., El-tantawi, A., and Mohamed, M. (2024). Evaluation of the air quality in arid climate megacities (Case study: Greater Cairo). *Contributions to Geophysics and Geodesy*, 54(1), 95-118.

Imane, S., Oumaima, B., Kenza, K., Laila, I., Youssef, E. M., Zineb, S., and Mohamed, E. J. (2022). A review on climate, air pollution, and health in North Africa. *Current Environmental Health Reports*, 9(2), 276-298.

Isaifan, R.J., Al-Thani, H.G. (2024). Action Taken to Reduce Air Pollution and Its One Health Impacts in MENA Countries. In: The Handbook of Environmental Chemistry. Springer, Berlin, Heidelberg.

Kyung, S., and Jeong, S. (2020). Particulate-matter related respiratory diseases. *Tuberculosis and respiratory diseases*, 83(2), 116.

Lamas, G. A., Bhatnagar, A., Jones, M. R., Mann, K. K., Nasir, K., Tellez- Plaza, M., . and American Heart Association Council on Epidemiology and Prevention; Council on Cardiovascular and Stroke Nursing; Council on Lifestyle and Cardiometabolic Health; Council on Peripheral Vascular Disease; and Council on the Kidney in Cardiovascular Disease (2023). Contaminant metals as cardiovascular risk factors: a scientific statement from the American Heart Association. *Journal of the American Heart Association*, 12(13), e029852.

Manisalidis, I., Stavropoulou, E., Stavropoulos, A., and Bezirtzoglou, E. (2020). Environmental and health impacts of air pollution: a review. *Frontiers in public health*, 8, 14.

Moawad, M. B., Youssief, A. A., & Madkour, K. (2017). Modeling and Monitoring of Air Quality in Greater Cairo Region, Egypt Using Landsat-8 Images, HYSPLIT and GIS Based Analysis. *Climate Change Research at Universities: Addressing the Mitigation and Adaptation Challenges*, 37-54.

Mohamed, M., Hwehy, M., Moursy, F., and El-tantawi, A. (2023). The synergy of ambient air quality and thermal discomfort: A case study of Greater Cairo, Egypt. *Journal of Agrometeorology*, 25(4), 553–559.

Monged, M., Imam, N., Aquilanti, G., Pollastri, S., Rashad, A., and Osán, J. (2022). Heavy metals concentrations and speciation of Pb and Ni in airborne particulate matter over two residential sites in Greater Cairo–reflection from synchrotron radiation. *Journal of synchrotron radiation*, 29(3), 765-774.

Rahman, Z., and Singh, V. P. (2019). The relative impact of toxic heavy metals (THMs) (arsenic (As), cadmium (Cd), chromium (Cr)(VI), mercury (Hg), and lead (Pb)) on the total environment: an overview. *Environmental monitoring and assessment*, 191, 1-21.

Safar, Z., and Labib, M. (2010). Assessment of particulate matter and lead levels in the Greater Cairo area for the period 1998–2007. *Journal of advanced research*, 1(1), 53-63.

Shetaya, W., El-Mekawy, A., and Hassan, S. (2024). Tempo-spatial Variability and health risks of PM2.5 and associated metal (loid) s in greater Cairo, Egypt. *Exposure and Health*, 16(4), 973-988.

Sivertsen, B. (2004). DANIDA. EIMP Phasing-out Phase, 2003-2004. A national air quality monitoring programme for EEAA, Egypt. *NILU OR*.

USEPA, (1999). Compendium method IO-2.3 Sampling of ambient air for PM10 concentration using the Rupprecht and Patashnick (R&P) low volume partisol sampler. Accessed on November 30, 2024 at https://www.epa.gov/amtic/compendium-methods-determination-inorganic-compounds-ambient-air

USEPA, (1999). Compendium method IO-3.4 Determination of metals in ambient particulate matter using inductively coupled plasma (ICP) spectroscopy. Accessed on November 30, 2024 at https://www.epa.gov/amtic/compendium-methods-determination-inorganic-compounds-ambient-air

WHO (2016). Ambient air pollution: a global assessment of exposure and burden of disease. WHO Press.

Vol. (54); No. (2); Feb. 2025
Print ISSN 1110-0826
Online ISSN 2636 - 3178

تقييم المعادن الثقيلة: الزئبق والرصاص والزرنيخ في الجسيمات الجوية في منطقة التبين السكنية، القاهرة، مصر

مروة عمر كسبر[1]– نبيل عبد القادر صالح[2]– محمود أحمد حويحي[1]
ناجا عبد الحميد أبو النيل[3]– وليد عبد الراضي حسان[3]

1) قسم العلوم الأساسية البيئية، كلية الدراسات والبحوث البيئية، جامعة عين شمس، القاهرة، مصر 2) قسم الكيمياء الحيوية، كلية العلوم، جامعة عين شمس، القاهرة، مصر 3) قسم الجغرافيا ونظم المعلومات الجغرافية، كلية الآداب، جامعة عين شمس، القاهرة، مصر

المستخلص

قامت الدراسة بتحليل البيانات وتفسير النتائج المستخلصة من دراسة تركيز المعادن الثقيلة في عينات الهواء التي تم جمعها على مستوى موسمي في ثلاثة مواقع سكنية مختارة بمنطقة التبين. انصبت الدراسة على تقييم المعادن الثقيلة للرصاص (Pb) والزئبق (Hg) والزرنيخ (As) في الجسيمات العالقة التي يبلغ قطرها الهوائي عشرة مايكرومتر أو أقل (PM10). وقد اعتمد العمل بشكل كامل على جمع 36 عينة هواء من المواقع المختارة، بمعدل 12 عينة في كل موقع خلال الفترة 2022–2023. كشف تحليل الجسيمات الجوية وتركيز المعادن الثقيلة في المواقع المختلفة عن وضع بيئي معقد. أظهر الموقع الأول تقلبات كبيرة في مستويات الجسيمات PM10، بينما شهد الموقع الثالث طفرات متقطعة، مما يشير إلى أحداث تلوث موسمية بهذين الموقعين. برز الزرنيخ بتركيزاته العالية في الموقع الأول مقارنة بالمستويات الأقل في الموقع الثاني. وقد أكدت الزيادة الملحوظة في الزئبق بهواء الموقع على تأثير الانبعاثات الناتجة عن حرق الفحم المستخدم كمصدر للطاقة في صناعة الأسمنت. في الوقت نفسه، أشارت المستويات المرتفعة للرصاص في الموقع الثاني إلى المصادر المحلية مثل الازدحام المروري والمسابك وأفران الصهر بالمنشآت الصناعية. لم تظهر تباينات كبيرة في تركيز الجسيمات PM10 في العينات المجمعة بالمواقع المحددة، ولكن التباينات في تركيزات المعادن الثقيلة كانت واضحة، مما يؤكد على ضرورة تبني الجهات البحثية والحكومية برنامج موسعا لإجراء تقييمات بيئية وتنفيذ خطط مواجهة مكثفة.

الكلمات المفتاحية: الجسيمات الجوية أقل من 10 مايكرومتر، المعادن الثقيلة في الهواء، الزرنيخ (As) ، الرصاص (Pb)، الزئبق(Hg) ، التبين، القاهرة.